Fabian Wolfertstetter[1]
German Aerospace Center (DLR),
Plataforma Solar de Almería,
Crtra Senés s/n,
Tabernas 04200, Spain
e-mail: Fabian.Wolfertstetter@dlr.de

Stefan Wilbert
German Aerospace Center (DLR),
Plataforma Solar de Almería,
Ctra Senés s/n,
Tabernas 04200, Spain
e-mail: Stefan.Wilbert@dlr.de

Jürgen Dersch
German Aerospace Center (DLR),
Linder Hoehe,
Cologne 51147, Germany
e-mail: Juergen.Dersch@dlr.de

Simon Dieckmann
German Aerospace Center (DLR),
Linder Hoehe,
Cologne 51147, Germany
e-mail: Simon.Dieckmann@dlr.de

Robert Pitz-Paal
German Aerospace Center (DLR),
Linder Hoehe,
51147 Cologne, Germany
e-mail: Robert.Pitz-Paal@dlr.de

Abdellatif Ghennioui
Institut de Recherche en Energie Solaire et
Energies Nouvelles (IRESEN),
Green Energy Park,
Km 2 Route Régionale R206,
Benguerir 43150, Morocco
e-mail: ghennioui@iresen.org

Integration of Soiling-Rate Measurements and Cleaning Strategies in Yield Analysis of Parabolic Trough Plants

The issue of reflector soiling becomes more important as concentrating solar thermal power plants (CSP) are being implemented at sites subject to high dust loads. In an operational power plant, a trade-off between reducing cleaning costs and cleaning related collector availability on the one hand and keeping the solar field cleanliness (ξ_{field}) high to minimize soiling induced losses on the other hand must be found. The common yield analysis software packages system advisor model (SAM) and greenius only allow the input of a constant mean ξ_{field} and constant cleaning costs. This oversimplifies real conditions because soiling is a highly time-dependent parameter and operators might adjust cleaning activities depending on factors such as soiling rate and irradiance. In this study, time-dependent soiling and cleaning data are used for modeling the yield of two parabolic trough plant configurations at two sites in Spain and Morocco. We apply a one-year soiling rate dataset in daily resolution measured with the tracking cleanliness sensor (TraCS). We use this as a basis to model the daily evolution of the cleanliness of each collector of a solar field resulting from the application of various cleaning strategies (CS). The thus obtained daily average ξ_{field} is used to modify the inputs to the yield analysis software greenius. The cleaning costs for each CS are subtracted from the project's financial output parameters to accurately predict the yield of a CSP project over its lifetime. The profits obtained with different CSs are compared in a parameter variation analysis for two sites and the economically best CS is identified. The profit can be increased by more than 2.6% by the application of the best strategy relative to a reference strategy that uses a constant cleaning frequency. The error in profit calculated with constant soiling and cleaning parameters compared to the simulation with variable soiling and cleaning can be as high as 9.4%. With the presented method, temporally variable soiling rates and CS can be fully integrated to CSP yield analysis software, significantly increasing its accuracy. It can be used to determine optimum cleaning parameters.
[DOI: 10.1115/1.4039631]

1 Introduction

The efficiency of concentrating solar power (CSP) plants depends on the reflectance of the concentrating mirrors. Their reflectance can be greatly reduced by soiling—the reversible process of particle and dust adhesion to surfaces. The parameter to quantify soiling-induced reflectance losses is called cleanliness (ξ). It is defined as the ratio of the reflectance (ρ) of a solar reflector relative to its reflectance in the clean state (ρ_{cl})

$$\xi(t) = \frac{\rho(t)}{\rho_{cl}} \tag{1}$$

the cleanliness changes due to time and site dependent on influences such as dust deposition, rain, and mirror cleaning. Depending on the CSP technology also, the cleanliness of entrance windows such as envelope tubes covering parabolic trough absorber tubes have to be considered. However, the effect of soiling on their transmittance is much lower than the effect on mirror reflectance as the small angle forward scattering induces a strong reduction of the specular reflectance, but only small reduction for the transmittance. Furthermore, the soiling layer has to be passed twice when reflected at second surface mirrors and only once when passing absorber tube glass envelopes, thus reducing the effect of the absorber tubes soiling effect. Cleanliness is often determined with handheld reflectometers by comparing the reflectance of the soiled mirror to that of a clean one [1]. In measurement campaigns, reflector samples are exposed to the environment and cleanliness is measured regularly. Often, the parameter soiling-rate (SR) is determined [2,3]. SR is defined as the change of cleanliness with time according to

$$SR(t) = \frac{d\xi(t)}{dt} \approx \frac{\xi(t + \Delta t) - \xi(t)}{\Delta t} \tag{2}$$

where Δt is the time difference between measurements. SR is typically a negative value and its absolute value is bigger when soiling occurs faster or soiling load is higher. Positive SR is found due to natural cleaning events such as strong rainfall. Long-term SR measurements for various sites have been reported [2,4–8]. They show high intra-annual variation of SR, which is mostly not bound to seasons. There is a strong dependence on the site of measurement

and the conditions of exposure such as inclination angle and orientation of samples [9]. Similar conclusions have been found for photovoltaic modules or cells [10–12].

There exist only few studies investigating the impact of SR and cleaning action on the financial yield of CSP plants. Reference [13] assumes a constant yearly SR in order to determine an optimal target cleanliness value that shall not be underrun during operation. The cost for one complete solar field cleaning in Ref. [12] is taken from Ref. [14] and the solar field size is one of the adjusted variables. They conclude that the optimal results with this cleaning strategy are obtained with a target cleanliness of 0.97–0.98 and a solar field 3–4% larger if cleanliness is assumed as 1.

References [1] and [15] determine an optimal cleaning frequency with only a few assumptions regarding cleaning costs (CC) and financial loss due to reduced reflectance. They use different constant SR to show that the resulting cleaning frequency is highly dependent on SR. They conclude that a constant monitoring of the average solar field cleanliness (ξ_{field}) is necessary for the best operation of a CSP plant [1].

All the above studies do not take into account the temporal variation of the SR and the cleaning frequency. This causes errors because, e.g., high direct normal irradiance (DNI) days might actually coincide with below average ξ_{field}. On a day with high DNI, a low cleanliness can reduce power plant output more (in absolute values) than on a cloudy day. The mentioned studies do not simulate plant yield in full detail but assume a linear correlation of plant output and cleanliness. This might cause further errors, for example if overload dumping plays a role. Overload dumping is necessary if the heat that could be provided by the solar field is higher than the heat that can be used by the power block and the storage together. In this case, collectors are defocused. In summer, overload dumping might mean that the same plant yield is obtained for a certain day regardless if cleaning has taken place or not.

To overcome these sources of errors, temporally variable SR and cleaning frequency are used combined with more detailed plant modeling software. The technical and financial output parameters of a CSP project over its lifetime can be calculated using yield analysis software such as *greenius* [16–18] or the system advisor model (SAM) [19]. Their calculations are based on a time-resolved meteorological dataset, the technical plant layout, and financial input parameters. The above-mentioned software products only offer the possibility to enter a constant yearly cleanliness value for the solar field to quantify soiling-induced losses. CCs are assumed as constant values per unit mirror area.

In the framework of this work, greenius was enhanced with an external software module that allows the treatment of time-resolved SR and cleaning including the corresponding collector outages and cleaning costs. We use this enhanced software to analyze cleaning decisions and its financial consequences in more depth for two parabolic trough plant configurations at two different sites. The following steps outline our approach:

(1) Apply a one-year SR dataset in daily resolution measured with the tracking cleanliness sensor (TraCS) [9,20,21] at Plataforma Solar de Almería (PSA) in the Tabernas desert in Spain.
(2) Model the cleanliness of each collector and thus $\xi_{field}(t)$ using the cleaning action of each cleaning unit (CU).
(3) $\xi_{field}(t)$ is used to modify the DNI dataset used as an input to *greenius*.
(4) Use realistic cleaning related cost parameters and calculate CC for each service hour and CU.
(5) Analyze the effects of different cleaning strategies (CS) and cleaning unit availability on plant yield output.

In the second section of this paper, we describe the input parameters for the modeling with a focus on the TraCS cleanliness measurements. Also, the financial and technical parameters used as inputs to *greenius* and CC calculation are presented. Section 3 describes the CSs and methodology to calculate CC and ξ_{field}.

Section 4 summarizes results; in Sec. 5 a sensitivity analysis is presented, and Sec. 6 contains conclusion.

2 Input Parameters

2.1 Meteorological Dataset. The yield analysis software *greenius* requires a meteorological dataset for one year. The first site that is investigated here is PSA in Spain (ES) located at 2.35 deg West, 37.1 deg North and 500 m above mean sea level. The second site is Missour, Morocco (MOR) located at 4.1 deg West, 32.9 deg North and 1107 m above mean sea level where a measurement station is run by IRESEN in cooperation with DLR [22]. The meteorological parameters applied in this study are DNI (direct normal irradiance) measured with pyrheliometers, global and diffuse horizontal irradiance measured with pyranometers, ambient air temperature, relative humidity, atmospheric pressure, wind speed and wind direction. These parameters are saved in 1-min resolution and averaged to hourly resolution. The same time interval from first of May 2013 until the Apr. 30, 2014 was evaluated for both sites. The data were quality checked on a daily basis following Refs. [23] and [24]. The DNI yearly sums for the sites used in the simulations are 2388 kWh/m²/a in ES and 2307 kWh/m²/a in MOR.

2.2 Soiling Rate Dataset. Reflectance and SR measurements with handheld devices are time-consuming and the time difference Δt in Eq. (2) between two subsequent measurements is usually in the order of days or weeks. This means that the resulting SR represents only a mean value in the measurement interval and is therefore not suitable for a daily modeling of soiling and cleaning in a solar field. In this study, we employ the TraCS. It is an automatic device that measures cleanliness in 10-min resolution by comparing the directly measured DNI to the DNI reflected by a sample mirror mounted on a solar tracker. The effective acceptance half-angle is 13.6 mrad and similar to a CSP collector [20,21]. The measurement area on the sample mirror is approximately 30 cm² in size. The SR is derived in daily resolution. The one-year SR dataset has been measured with TraCS at PSA. The sample mirror has been cleaned approximately every 2 weeks. In the measurement period, the cleanliness of the sample mirror never dropped below 0.82. The SR dataset is shown in Fig. 1. The average SR is −0.0052/d with a standard deviation of ± 0.0095/d and the highest SR is −0.089/d. Positive SR values are due to rain cleaning of the sample mirror and are also considered in the cleaning simulations. SR varies significantly throughout a year. The assumption of a constant SR made in previous studies therefore seems unrealistic.

2.3 Power Plant Layouts. Two different layouts of parabolic trough power plants are used in this analysis. Their specifications are shown in Table 1. The two layouts are chosen following the
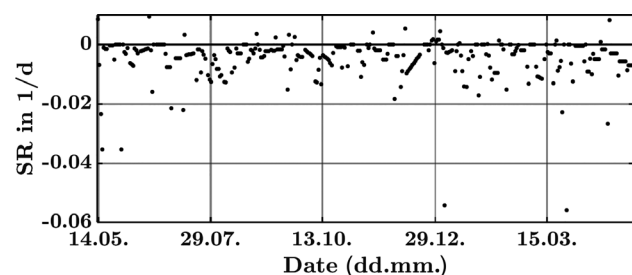

Fig. 1 Soiling rate SR in daily time resolution measured with TraCS at PSA from May 2013 until May 2014. The mirror was cleaned roughly every 2 weeks. Negative values represent a decrease in cleanliness from one day to the next, and positive values are caused by rain events. One measurement value from the Feb. 16, 2014 with SR = −0.089/d is not shown for scaling reasons.

Table 1 Technical data for the two parabolic trough power plants used as templates for the plant layouts used in this study. The solar field size is linearly scaled according to the DNI yearly sums at the sites ES and MOR.

Parameter	Andasol I template for AS	Ibersol Puertollano template for IP
Nominal turbine power	49.9 MW	49.9 MW
Collector type	Euro Trough 150	Euro Trough 150
Number of loops	156 (140 in ES, 144 in MOR)	88 (76 in ES, 78 in MOR)
Aperture area of solar field at the original plant site	510,000 m^2	287,000 m^2
Thermal storage	7.5 h	None
Cooling technology	Wet cooling tower	Wet cooling tower
Investment cost (without cleaning units)	ca. 310 MEUR	ca. 200 MEUR
Staff at operation (excluding cleaning personnel)	40	31
Projected lifetime	25 years	25 years
DNI yearly sum at original site of template plant	2136 kWh/m^2/a	2061 kWh/m^2/a
DNI yearly sum for sites in simulations	2388 kWh/m^2/a in ES and 2307 kWh/m^2/a in MOR	

Table 2 Overview of the cost parameters for MOR and ES used as an input to *greenius*. The percentage values in the specific cost parameters refer to the total investment cost of the solar field.

Parameter	MOR	ES	Unit	Source
Price of land	1.5	2	EUR/m^2	Estimations based on Ref. [26] (MOR), [27,28] (ES)
Interest rate	6.0	3.2	%	[29] (MOR), [30] (ES)
Specific investment cost solar field	275	300	EUR/m^2 [a]	Estimation based on Ref. [31]
Equity ratio	30	30	%	Estimation based on Ref. [31]
Specific replacement cost	1	1	%/a	Estimation based on Ref. [31]
Specific insurance cost	0.7	0.7	%	Estimation based on Ref. [31]
Specific operation cost	1.8	2.5	EUR/m^2 [a]	[31] for ES
Feed in tariff	0.18	0.27	EUR/kWh$_{el}$	[32] (MOR), [33] (ES)[b]

[a]The m^2 unit refers to the collector aperture area, not the mirror surface in all specific cost parameters.
[b]Source from 2013. The slight modification of the Spanish feed-in tariff of 2014 has been ignored in this study. It will not change significantly the presented exemplary results.

power plants "Ibersol Puertollano" (IP) and Andasol I (AS) [25]. They both dispose of a turbine with a nominal electrical output of 49.9 MW$_{el}$. AS has a thermal storage capacity of 940 MWh$_{th}$, or 7.5 h full load turbine operation while IP has no storage.

The solar fields were scaled linearly such that the product of DNI yearly sums and number of loops is approximately equal for the original (template) and target sites of ES and MOR. The power plants are operated following the strategy "solar only." This strategy prioritizes the full load operation of the turbine: As long as there is not enough thermal output from the solar field, the missing thermal energy is taken from the storage. If there is more thermal output from the solar field, the excess heat is transferred to the storage in the case of available storage capacity in AS. If storage is fully loaded or absent, the excess heat needs to be discarded (overload dumping). Keeping the storage medium above freezing temperature has priority over electricity generation.

2.4 Financial Data Including Cleaning Costs. Financial parameters are required by *greenius* to calculate the financial output of CSP projects and to quantify CC for each CS. The site-specific financial parameters for ES and MOR are listed in Table 2. The parameter "Specific operation costs" does not include CC.

The inflation was set to zero in the *greenius* calculations. This is an approximation that is assumed to be compensated by the fact that also no cleaning efficiency increase is considered. Such an increase is very likely especially because new and improved vehicles will be bought after the assumed lifetime of the first vehicles of 15 years. It is assumed that this effect counterbalances inflation.

The parameters used as a basis for the CC calculations are shown in Tables 3 and 4. The cleaning unit (CU) specification in Table 3 is used to determine the consumption of fuel, water, and

personnel. The parameters cleaning speed and cleanliness after cleaning (ξ_0) have been determined in a field test described in Ref. [34]. ξ_0 is not equal to 1 because cleaning is not perfect in general. It also includes the influence of mirror sections that cannot be reached by the CU. These are left dirty and account for roughly 4% of the mirror surface. The cleaning speed includes the time needed to rank at the collector edges, to refill the water and fuel tank, and to reach the garage and refill stations.

The cost parameters in Table 4 are used to convert the technical parameters to financial values. The yearly salary per person refers to gross costs for the industrial sector. Only those hours spent with cleaning are included in CC calculations. This means that the worker takes on additional tasks in operation and maintenance of the solar field. The wage for short-term workers that can be hired to clean the mirrors manually without the cleaning vehicle is assumed as 150% of the obligatory minimum wage. The depreciation cost of the CU has been calculated as an annuity loan over its assumed lifetime using the countries' interest rates. Annuity loan is characterized by constant down-payments during the amortization period, similar to a leasing model.

Table 3 Specifications of the cleaning vehicle model "Albatros" [35] chosen for the simulations. Most data have been taken from Ref. [34]. All parameters are given for one vehicle (also called unit).

Cleaning speed (R_A)	9 loops per 8 h shift
Operating staff	1 person
Fuel consumption	6–8 l/loop
Cleanliness after cleaning (ξ_0)	0.986
Capacity of the water tank	5 m^3
Water consumption (demineralized)	0.3 l/m^2
Assumed lifetime	15 a

Table 4 Cost parameters related to cleaning activities

Cost parameter	MOR	ES	Unit	Source
Salary for 1 person-year (K_L)	6725	48,000	EUR/person-year	[36] (MOR) [37] (ES)
Wage for short term workers (K_L^{as})	1.5	7	EUR/h/person	[38] (ES), [39] (MOR)
Water cost	0.36	0.39	EUR/m^3	[40] (MOR), [34] (ES)
Fuel cost	1.1	1.5	EUR/l	[41]
Depreciation CU (K_{CU})	58,300	51,400	EUR/CU/a	Price estimation from [34], depreciation calculated as annuity loan with country specific interest rate

3 Cleaning Strategies and Calculation of Cleaning Effects

This section describes the method to trace the CU movement throughout the year following several sets of rules called CS and the procedure to calculate the resulting CC and daily ξ_{field}.

3.1 Cleaning Strategy Definitions. We define two different types of CS: two different threshold-based CSs, where the cleaning intensity is adapted to the current ξ_{field} and constant CSs where cleaning occurs at a fixed frequency. The motivation for the threshold-based CSs is to reduce CC whenever ξ_{field} is sufficiently high.

A summary of the CSs is given in Table 5. The following assumptions apply:

(1) One cleaning shift (day or night) lasts 8 h.
(2) Cleaning during the day implicates defocusing of the currently cleaned loops resulting in lower solar field availability
(3) If more than one CU is used, each pair of two CUs cleans the same loop simultaneously to maximize availability.
(4) The labor for measuring ξ_{field} is not accounted for in CC calculation. This is part of the specific operation costs in *greenius*.
(5) In the strategies "Threshold" and "Assisted," either all or none of the CUs take up cleaning if ξ_{field} is below the threshold ξ_{lim}. If ξ_{field} falls below $\xi_{\text{lim, as}} < \xi_{\text{lim}}$, additional four cleaning teams of short-term workers for manual cleaning are hired in the CS Assisted.

Each cleaning team consists of four additional workers that use manual wipers to clean the mirrors. The investment cost for the additional cleaning teams' gear is neglected. The cleaning speed of each additional team is half the speed of a CU consuming half the amount of water per loop as a CU and negligible amounts of fuel. The external workers are employed in two daily shifts until $\xi_{\text{field}} > \xi_{\text{lim}} - 0.01$.

The following parameters are varied within the limits given below:

(1) Number of available CUs in the solar field (N_{CU}) from 1 to 6.
(2) ξ_{lim} for the strategies Threshold and assisted from 0.96 to 0.99.
(3) Power plant type IP/AS.
(4) Location ES/MOR.

For each combination of parameters, a simulation run for one-year power plant operation is performed. To keep the results manageable, only $\xi_{\text{lim, as}} = 0.9$ is used for the second threshold in the CS Assisted in this study. This choice follows the recommendation to keep ξ_{field} constantly above this value [4]. Also, we only model a fixed number of four external cleaning teams that assist the CUs of the power plant in case that $\xi_{\text{field}} < \xi_{\text{lim, as}}$.

3.2 Cleaning Cost Calculation. CC for each case is determined in two steps, first the specific costs in units of EUR per loop are calculated from the values listed in Tables 3 and 4. The labor cost for an assisting cleaning team of four people for one loop is calculated according to

$$P_L^{as} = K_L^{as} \cdot (4 \text{ persons})/R_A^{as} \tag{3}$$

where K_L^{as} is the cost for one working hour and $R_A^{as} = R_A/2$ the number of loops that are cleaned in one hour. Accordingly, the labor cost to clean one loop with a CU is calculated as

$$P_L = \frac{K_L \cdot 1 \ [\text{person} - \text{year}]}{R_A \cdot 250 \cdot 8\text{h}} \tag{4}$$

K_L is the yearly cost of a solar field worker according to Table 4. The conversion from person-year to costs per hour is obtained assuming 250 work days of 8 h in a person-year.

Fuel cost P_F and water cost P_W per loop cleaning are determined by multiplication of the respective values in Tables 3 and 4. For the yearly cleaning costs, the following equation applies:

$$\text{CC} = N_{\text{CU}} \cdot K_{\text{CU}} + \sum_{d=1}^{365}(P_L + P_F + P_W) \cdot N_{l,\text{cl}}(t_d)$$
$$+ \sum_{d=1}^{365}(P_L^{as} + P_W^{as}) \cdot N_{l,\text{cl}}^{as}(t_d) \tag{5}$$

with K_{CU} being the depreciation cost per CU. $N_{l,\text{cl}}$ is the number of loops cleaned with CUs on each day t_d. The superscript "as" marks costs for additional cleaning teams in CS assisted. Thus, the last term in Eq. (5) does not apply for CSs threshold and constant.

3.3 Determination of Solar Field Cleanliness and Availability. In order to determine $\xi_{\text{field}}(t)$, $N_{l,\text{cl}}$, and $N_{l,\text{cl}}^{as}$, the cleaning action of each CU and the cleanliness of each trough (ξ_i) are

Table 5 CS and their short descriptions. The mode parameter indicates when cleaning is performed: *n* stands for nightly cleaning and *dn* for cleaning in one day and one night shift.

CS name	Mode	Short description	Frequency
Constant	*n*	Clean at a constant rate only during the night shift with all available CU	Fixed
Constant	*dn*	Clean at a constant rate during day and night shifts. This is the reference strategy when 1 CU is utilized.	Fixed
Threshold	*n/dn*	Clean with all CU only if ξ_{field} is lower than a threshold ξ_{lim}	Variable
Assisted	*n/dn*	Similar to threshold, but additional manual cleaning teams are hired if ξ_{field} falls below a second threshold value $\xi_{\text{lim, as}} < \xi_{\text{lim}}$.	Variable

modeled in an external software add-on for greenius. It is assumed that the same SR applies equally to each loop of the solar field as long as it is not cleaned

$$\xi_i(t_d + 1d) = \xi_i(t_d) + SR(t_d) \cdot 1d \qquad (6)$$

where t_d represents the day of the year, d is the time unit day, and ξ_i refers to the cleanliness of loop number i. Each CU takes up cleaning at the beginning of one shift where it stopped at the end of the last shift. This way, the loops that have been exposed longest to soiling are cleaned first. The loops of the solar field are cleaned in the same order. Once a CU has reached the end of the field, it starts from the first loop again. External cleaning teams follow the same order. They are distributed in a way that the number of loops separating the cleaning vehicles and teams is as homogeneous as possible.

The cleanliness $\xi_{i,cl}$ of those loops that have been cleaned during the night shift before sunrise on day t_d is set to $\xi_0 = 0.986$, as given in Table 3. If cleaning is performed during daytime, the mirrors are used partly in the dirty state and partly in the clean state before and after cleaning, respectively. This leads to the following simplified equation for mirrors that are cleaned on the day t_d:

$$\xi_{i,cl}(t_d) = \begin{cases} \xi_0, & \text{if nightly cleaning} \\ \dfrac{\xi_0 + \xi_i(t_d)}{2}, & \text{if daytime cleaning} \end{cases} \qquad (7)$$

Because only daily mean values for ξ_{field} are calculated, the difference in clean and dirty exposure times among the different cleaned troughs are assumed to cancel out. On the following day

$$\xi_{i,cl}(t_d + 1d) = \begin{cases} \xi_0 + SR(t_d) \cdot 1d & \text{if nightly cleaning} \\ \xi_0 + SR(t_d) \cdot 0.5d & \text{if daytime cleaning} \end{cases} \qquad (8)$$

is used for all troughs cleaned on day t_d. This adjustment accounts for the longer exposure time of the loops that were cleaned during the night preceding the day t_d compared to the shorter exposure time of the loops subjected to daytime cleaning.

Finally, the daily mean solar field cleanliness is calculated according to

$$\xi_{field}(t_d) = \sum_{i=1}^{N_{loops}} \xi_i(t_d) / N_{loops} \qquad (9)$$

with N_{loops} being the number of loops in the solar field.

In a next step, the availability S due to daytime cleaning in the solar field is determined. First, the availability S_i of each loop i is calculated

$$S_i(t_d) = \begin{cases} 1, & \text{if no or nightly cleaning} \\ 1 - \dfrac{T_{cl}}{T_d(t_d)}, & \text{if cleaned during daytime} \end{cases} \qquad (10)$$

where T_{cl} is the time when the CU or a pair of two CUs needs to clean one loop and $T_d(t_d)$ being the length of the solar day, i.e., the time between sunrise and sunset on day t_d. The length of the solar day is halved if a pair of two CUs cleans the same loop simultaneously.

Finally, the average of the $S_i(t_d)$ for all loops and $\xi_{field}(t_d)$ are multiplied to every hourly DNI value of day t_d according to

$$DNI_{mod}(t) = DNI(t) \cdot \xi_{field}(t_d) \cdot S(t_d) \, \forall t \in t_d \qquad (11)$$

where t represents time in hourly resolution and t_d the day of the year. This equation applies to all days t_d of a year.

The hourly one-year modified DNI time series (DNI_{mod}) is then passed as an input to greenius instead of the original DNI measurement data. A reduction of DNI is assumed to have the same effect on solar field thermal output as a reduction of mirror cleanliness. The parameter ξ_{field} in greenius is not used, i.e., it is set to 1 in all our simulation runs.

3.4 Comparative Parameters. This study focuses on comparing different CSs among each other. Therefore, a reference CS is chosen as "Constant dn" using one CU during one daily and one nightly shift. The financial performance of any candidate CS is compared to the performance of this reference CS.

Greenius returns several financial and technical output parameters. In order to obtain a meaningful parameter for the direct comparison of CSs, a financial parameter has to be used. The average dividends per year paid during the lifetime of a plant (D_y) are used here as a basis for a comparative parameter. D_y represents the average profit for investors over the 25 year project duration, i.e., the average yearly revenues from electricity sales minus average yearly costs for operation (incl. cleaning), replacement, insurance, debt service. The yearly dividend varies during the project lifetime: It is negative during construction phase and increases steadily until all loans have been paid off. Variation caused by different DNI datasets is excluded in this study since the same meteorological year is used for all simulated years. Here, we calculate the mean annual net dividends (D_y) as

$$D_y = (D_{wocl}/T_{lt}) - CC \qquad (12)$$

where D_{wocl} is the total dividend without considering cleaning costs, T_{lt} is the lifetime of the project, and CC is the yearly cleaning cost as defined in Eq. (5). Normalizing D_y to the net dividends achieved by application of the reference cleaning strategy ($D_{y,ref}$) leads to the relative profit increase (RPI) defined as

$$RPI = \left(\frac{D_y}{D_{y,ref}} - 1 \right) \cdot 100\% \qquad (13)$$

The RPI is used in the following as the main comparative parameter. The absolute net profit increase (API) is calculated as

$$API = D_y - D_{y,ref} \qquad (14)$$

4 Results and Discussion

Some of the financial output parameters for the reference strategy (Constant dn, with one CU) and the strategy "Threshold n" with three CUs are given in Fig. 2 for AS in ES. The difference in the total revenues and profit of the project show small relative differences. The higher cleaning intensity in Threshold n increases the CC by a factor of 2 and ξ_{field} by 1%. Water costs are displayed on a scale of factor 100 smaller than the other parameters that contribute to CC.

The CC account for 6.6% of the running costs and 12.5% of the operation and maintenance (O&M) costs (both including CC) in the example CS (Threshold n). Approximately, half as high values are found for the reference CS. The CC corresponds to 1–3% on the annual profits of the project. The 1.3% increase to 3262 turbine full load hours causes an increase of 0.18% of O & M costs. The example CS results in an RPI of 0.76% and an API of 122 kEUR/a with D_y being 16.1 MEUR/a. The power plant produces 1.7 GWh$_{el}$/a or 1.2% more electrical energy if the example CS is applied in comparison to the reference CS. Total revenues differ by the same percentage or 463,000 EUR/a. The project amortizes economically 2.3 months earlier. The LCOE (levelized costs of electricity) is 0.1806 EUR/kWh$_{el}$ for the reference CS and 0.1790 EUR/kWh$_{el}$ for the example CS. CC have not been accounted for in the LCOE.

4.1 Results of the Constant Cleaning Strategy. The RPI is calculated for the four combinations of countries (ES and MOR) and power plant layouts (AS and IP). The RPIs are plotted in
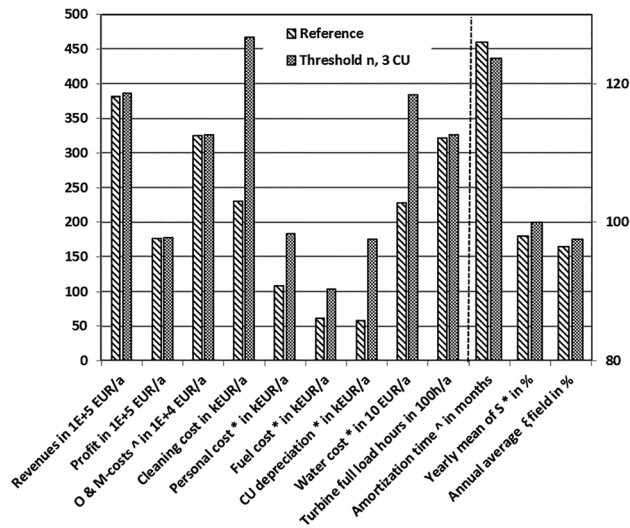
Fig. 2 Overview of selected output parameters from _greenius_ and cleaning cost calculation for plant type AS in ES and two example cleaning strategies: Constant _dn_ (reference CS) and Threshold _n_ with 3 CUs. Units are given in the column titles, and the dashed line separates affiliation to the two Y-scales. The scale of the three right parameters is shown on the right and that of the rest on the left. Values marked with * refer to cleaning specific costs, the calculation of those marked with ˆ do not include cleaning activities.

Fig. 3 against N_{CU} for both modes n and dn. In Figure 3 left, results for AS are shown and results for IP are shown on the right. The maximum RPI of 1.35% is reached for AS in MOR with $N_{CU} = 2$ and mode dn. This CS results in an API of 141 kEUR/a. The occurrence of the maximum for AS, MOR, and this CS can be explained by the fact that the availability of the solar field is the same as in the reference CS because of the pairing of even numbers of CUs. Cleaning intensity, i.e., the number of loops being cleaned per day, is doubled at the same time with only one more CU in service. Larger steps occur when going from even to uneven N_{CU}. This effect is attributed to the unsteady decrease of the availability S that is not present when going from uneven to even N_{CU} because of pairwise cleaning with two CUs of one loop. In comparison to the mode n with three CUs, S is smaller but one CU more has to be financed, resulting in higher CC. The

difference to the maximum RPI in MOR and cleaning mode n is relatively small: RPI is 1.26% with 3 CUs compared to 1.35% for the maximum for MOR found with Constant n.

For ES, the maximum RPI is 0.53% and API is 84.3 kEUR/a deploying 3 CUs that operate in nightly shifts. D_y in this case is 16.1 MEUR/a. The CS Constant tn peaks at an RPI of 0.12% or an API of 18.5 kEUR/a when employing two CUs.

In the power plant IP (Fig. 3, right), the following observations are made: The maximum RPI occurs for both countries for the cleaning mode n with two CUs. The maximum RPI is 0.91% in ES and 0.82% in MOR. The cleaning intensity for this CS is the same as in the reference CS (Constant dn, 1 CU). The positive RPI is caused by the higher availability S that overcompensates for the higher CU depreciation cost.

The cleaning mode tn does not result in a positive RPI in IP. The reference CS with one CU is the best configuration for this cleaning mode. For greater N_{CU}, the RPI in IP decreases faster than in the left graph (AS). This behavior can be explained by the smaller solar field in IP where S assumes lower values for same N_{CU} than in AS.

Labor costs for night shifts are assumed to be the same as for day shifts in this study. An increase of 25% on costs for night labor as is recommended for Germany [42] would still lead to the finding that the highest RPI are reached with nightly cleaning. As there is no reliable information available on the implementation of such an increased night shift salary for countries like Morocco, the comparability of the two sites would be compromised and therefore an increased night salary is omitted.

In summary, nightly cleaning is more profitable than cleaning in day and night shifts. The profit of a project can be increased by up to 1.35% if the optimum number of CUs and constant nightly cleaning is selected.

4.1.1 Effect of Cleaning Strategies on Dumping. The defocusing of a part of the solar field when thermal output exceeds the capabilities of the power block and the storage is called dumping. A higher ξ_{field} increases the optical efficiency and thus the thermal energy produced in the solar field which in turn increases dumping.

The thermal energy that is not collected due to dumping is called Q_{dump}. In Fig. 4, the ratio of Q_{dump} and the total thermal energy if no dumping would be required (Q_{tot}) is plotted against N_{CU} for the CS Constant in all countries and power plants. With increasing N_{CU}, ξ_{field} increases. Therefore, Q_{dump} also increases steadily for the cleaning mode n because the threshold for dumping of the thermal solar field output is reached more frequently than with a lower ξ_{field}. Because Q_{tot} also depends on ξ_{field}, this
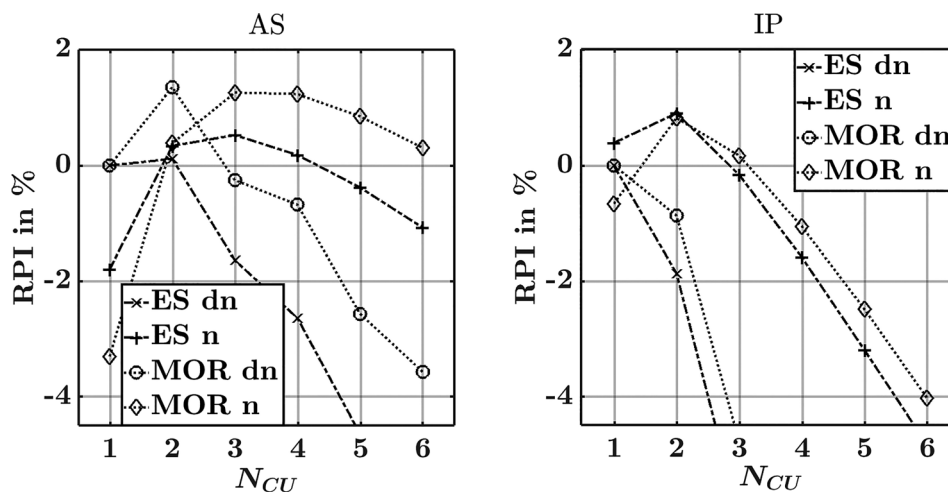

Fig. 3 RPI plotted against N_{CU} for all configurations of the CS "Constant". RPI compares the candidate CS to the reference strategy (Constant _dn_ with one vehicle) for the same countries and power plants. Left for the power plant AS, right for the plant IP. _dn_ means that cleaning is performed in one daily and one nightly shift, _n_ means only one nightly cleaning shift.
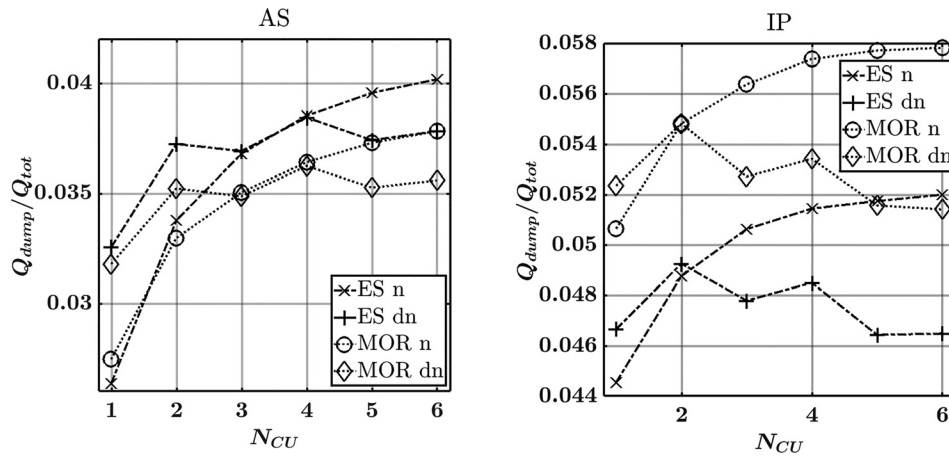
Fig. 4 Ratio of dumped potential thermal power Q_{dump} and total potential thermal power Q_{tot} plotted against N_{CU} for both power plant types and sites for CS Constant *n* and *dn*

increase is not linear. $Q_{\text{dump}}/Q_{\text{tot}}$ behaves differently in the cleaning mode *tn* due to the properties of the solar field availability S that can also be seen in Fig. 3.

The effect of cleaning on $Q_{\text{dump}}/Q_{\text{tot}}$ raises the question if it could be incorporated into cleaning decision-making. In theory, it would be better to omit cleaning some days before a period with excess solar insolation in order to save running cleaning costs. From a practical point of view, this would require a reliable forecast of the irradiance and the soiling rate for the next days, because ξ_{field} cannot be altered instantaneously, i.e., it takes several days to clean a solar field completely. While DNI forecasts are available, the soiling rate is currently not forecasted. Persistence forecast could be applied in combination with rain and dust storm forecasts, but this is not considered in this study.

4.2 Results for the Strategy Threshold. The CS Threshold is similar to the CS Constant with the difference that if ξ_{field} is greater than a threshold value ξ_{lim}, the CUs stop cleaning in order to reduce CC. In the following, N_{CU} and ξ_{field} are varied. Only nightly cleaning is considered, because it showed better performance in the constant cleaning strategies.

The resulting RPIs are displayed in a color-coded 2D plot shown in Fig. 5. The location of the maximum RPI is marked by an "X" with the value displayed next to it.

The RPIs shown in the uppermost row of each graph correspond to the RPIs shown in Fig. 3 for CS Constant *n* and same combinations of power plant, country, and N_{CU}. The reason is that ξ_{lim} is greater than the cleanliness after cleaning $\xi_0 = 0.986$ there. This causes the CUs to clean the solar field every night. If an RPI at $\xi_{\text{lim}} < \xi_0$ is greater than the RPI in the uppermost row, the application of CS Threshold can increase the profit of the project for same N_{CU}.

In power plant AS in MOR, the highest RPI of 1.36% is found for $\xi_{\text{lim}} = 0.99$. Hence, no increase of RPI is achieved by application of the CS Threshold in comparison to CS Constant. For IP in MOR, the maximum RPI can be increased by 0.16% to 0.98% for $N_{\text{CU}} = 2$. Here and in the following, the percentage values used for comparing RPIs are to be understood as absolute increases. In IP in ES, the CS Threshold leads to an increase in maximum RPI of 0.36% to 1.27%. Generally, the difference between the CSs Threshold and Constant are greater for the power plant IP due to the higher effect of CC on net profit.

In ES, the possible CC reduction due to the application of CS Threshold is higher compared to MOR, because of higher personnel rates and material costs. The increase of maximum RPI with CS Threshold is 0.23% compared to CS Constant in ES. The

running cleaning costs are more than 65 kEUR/a or 16% lower compared to CS Constant.

The gradient of the RPI in the proximity of the maximum RPI is smaller in AS compared to IP. One of the reasons is the higher N_{CU} at the peak RPI in AS: A difference of one vehicle causes less relative difference in CC and cleaning intensity. In MOR, the gradients are higher than in ES due to the higher ratio CC/D_y. This implies that a change in CC has more effect on the projects' net profit. The same changes in CC thus have more effect on RPI in MOR than on the RPI in ES.

It can be concluded that the application of the CS Threshold can increase the RPI by up to 0.36% relative to the CS Constant. It is therefore attractive for power plant operators to monitor ξ_{field} and base their cleaning decisions upon it.

4.3 Results for the Strategy Assisted. The resulting maximum RPIs for the CS Assisted and the soiling rate time series used so far are identical to those for CS Threshold. Therefore, the RPIs are not shown here for the application of the CS Assisted. The reason is that ξ_{field} never falls below the second threshold value $\xi_{\text{lim}}^{\text{as}} = 0.9$ at the points where the maximum RPI is reached. In this case, no external personnel are hired resulting in the same cleaning action for both CS. For combinations of ξ_{lim} and N_{CU} for which RPIs below the maximum RPI are reached, the external personnel play a role. The effect of the CS Assisted is found in the significantly lower gradients when moving away from the point of maximum RPI in direction of N_{CU} and/or ξ_{lim}. Thus, the CS Assisted is more robust to wrong cleaning decisions even if no increase of the maximum RPI is achieved.

4.3.1 Soiling Scenario With Five Heavy Soiling Events. In order to investigate the effects of different CSs at a site subjected to more severe soiling conditions, the SR dataset measured at PSA is altered by the introduction of five heavy soiling events as could be caused by sand storms or aerosol wet deposition events. The SR values and days are created randomly to −0.21, −0.10, −0.15, −0.11, and −0.22 per day for the days of the year 31, 49, 158, 166, and 302.

The results of the simulation runs for the CS Threshold and Assisted for this altered soiling rate time series are shown for the power plant AS in Fig. 6. The maximum RPIs roughly double for both CS compared to the results for the original soiling rate data set. The maximum RPIs for CS Threshold are achieved with one more CU compared to the original SR dataset. This can be explained by the fact that the higher SRs cause lower power output for the cleaning intensity applied in the reference CS. Employing more CUs can compensate better for the soiling induced losses.
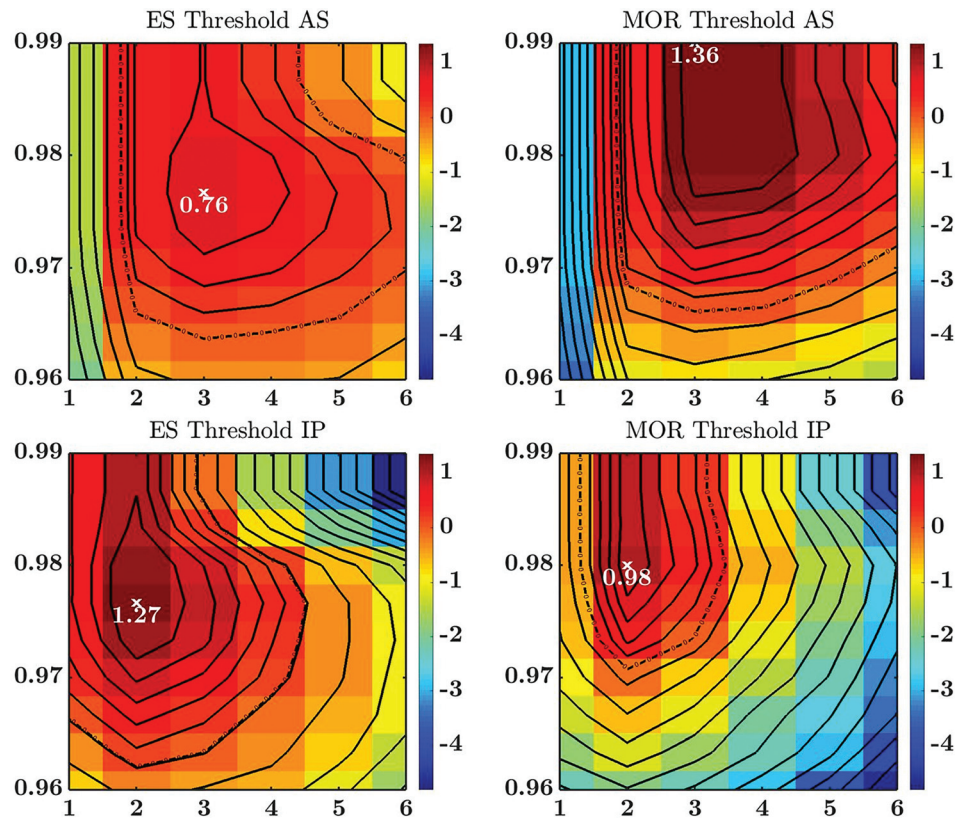
Fig. 5 Comparison of RPI for CS Threshold where color represents the RPI in %. The *x*-axes values represent N_{CU}, the *y*-axes represent ξ_{lim}. Power plant AS is shown in the upper graphs and IP in the lower graphs. In the left column, financial values from ES have been applied and in the right column those from MOR are used. The color scale is the same in all graphs. Each color tile represents one simulation run with the exact parameter combination at the center of the tile. The step width for the parameter variation is 1 for N_{CU} and 1/300 for ξ_{lim}. The contour lines are shown as an orientation. The dashed contour line represents RPI = 0.

In all cases, the here applied CSs perform better than the CS Constant. The CS Assisted reaches very similar maximum RPIs with the difference that one CU less is employed. Due to the labor costs, CS Assisted reaches slightly lower RPIs in ES than in MOR. The gradients of RPI are less pronounced in the CS Assisted qualifying this strategy are more robust against an imperfect choice of N_{CU} or ξ_{lim}. The CS Assisted can also help to avoid losses in years when untypically high soiling rates occur, for which the number of CUs present in the power plant are not sufficient. For example, if a lower number of three CU*s* and a ξ_{lim} of 0.987 are applied in AS in MOR, an RPI of 1.87% is achieved with CS Threshold compared to a RPI of 2.10% with the CS Assisted. Similar differences are found for most other points in the graphs.

4.4 Evaluation of the Errors Caused by the Assumption of Constant Cleaning Parameters. In the following, it is investigated how accurate simulations with the assumption of constant soiling rates or even cleanliness are. Such approximations simplify the modeling. Furthermore, it must be considered that soiling rate time series are currently not available for most sites and the estimation of an average soiling rate is easier to obtain than time series.

4.4.1 Cleaning Strategy Threshold at a Constant Soiling Rate. In the following, the CS Threshold is applied to a scenario of a constant SR equal to the mean value of the PSA data set of −0.0052 per day. The reference CS yield was also calculated for this constant SR. Figure 7 shows that the maximum RPI is 0.21% smaller for this scenario compared to the original SR dataset (see

Fig. 5). The CS Threshold cannot increase profits in comparison to SR Constant for this scenario.

If the SR of a site is approximated by one constant value for all days of the year, the best number of CUs and cleaning mode can be determined sufficiently for the CS Constant in this case. A potentially higher RPI for fluctuating SR and advanced CSs cannot be detected. For the best planning of cleaning action and the best estimation of financial project outputs, time-resolved SR measurements are therefore recommended.

4.4.2 Assumption of a Constant Solar Field Cleanliness. In many existing studies, a constant ξ_{field} of 0.95 is assumed [43–46]. The average value of ξ_{field} resulting from the application of the reference CS to the original SR dataset is 0.965 with a standard deviation of 0.013. The reference CS (calculated with the original SR dataset) achieves a profit that is 2.2% higher than the one achieved with $\xi_{field} = 0.95$ even if CC are set to 0 for the constant cleanliness scenario. If the CC for the case of a constant ξ_{field} is set to the same value as resulting from the reference CS, the difference in profits is 9.4%. The assumption of a constant ξ_{field} can thus cause significant errors.

If the average cleanliness for the reference CS and the soiling time series (0.965) is set as the constant ξ_{field} and the same CC as in the reference CS are used, the constant scenario results in a profit that is 0.58% higher than the one obtained with the original SR and reference CS. This difference is caused by the variation of ξ_{field}, the solar position-dependent plant efficiency and DNI variation in the course of the year. Therefore, different ξ_{field} values are weighted differently by the plant efficiency and DNI occurring at different days. This means that in the reference case, ξ_{field} on
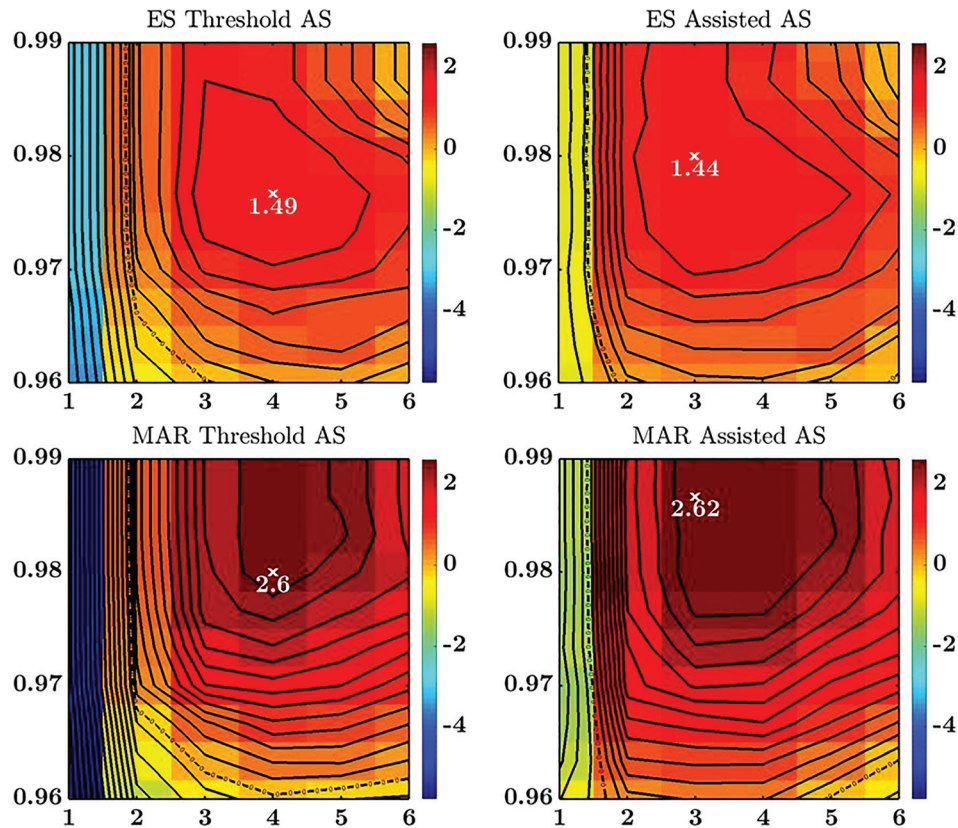
Fig. 6 Comparison of the CS threshold and assisted for AS in Spain and Morocco. The simulations were performed with the SR data set that has been extended by five randomly created intense soiling events. The RPI shown in color was calculated in comparison to the reference CS applied to the same soiling rate scenario. The color scale is the same for all graphs. Strategy, power plant type, and site are shown in the headers.

average was lower on days with higher used DNI. Thus, if a constant ξ_{field} is applied and is estimated in the best possible way for yield analysis, the remaining uncertainty will be in the range of 0.58%.
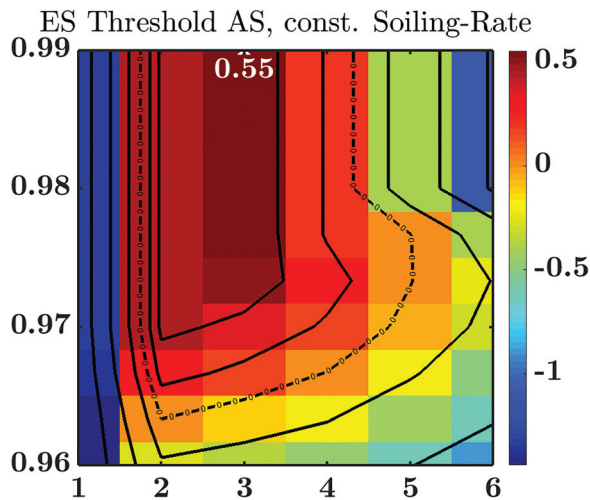

Fig. 7 Simulated RPIs shown in color for the CS threshold in ES and AS, where the x-axis shows the number of CU employed and ξ_{lim} is shown on the y-axis. The soiling-rate dataset used was set to the average soiling rate of −0.0052/d of the dataset acquired at PSA for every day of the year. The depicted scenario is the same as shown in the upper left graph of Fig. 5 with the only difference that here the SR has been assumed as constant in time with the mean value of the measured SR from PSA here.

5 Sensitivity Analysis

The influence of the input parameters on the RPI is investigated in the following. The parameters from Table 4 as well as the lifetime of the CUs, the feed-in tariff, and the mean SR are varied while keeping the rest of the inputs at their original values. The effects on the RPI obtained with the SR Threshold with $N_{\text{CU}} = 3$ and $\xi_{\text{lim}} = 0.977$ in AS in ES are shown in Fig. 8. The average of the SR dataset is the most influential of the parameters if varied from 50% to 150% of their initial values. The SR was varied by simple multiplication of each daily value with a constant factor.

The feed-in tariff has the greatest influence on the RPI among the financial input parameters followed by the prices applied in the calculation of CC. The influence of the latter roughly corresponds
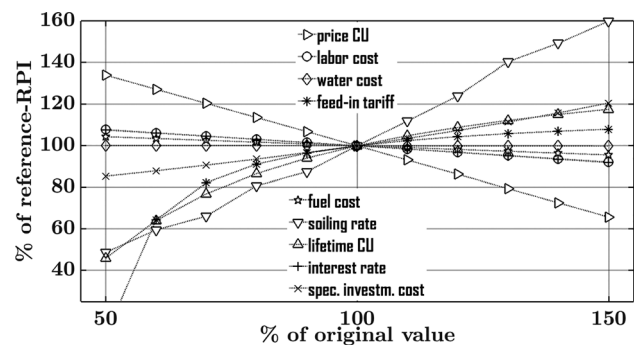

Fig. 8 Influence of the financial and some technical input parameters on the RPI of the CS threshold with 3 CUs and a ξ_{lim} of 0.977. Original values are those given in Tables 1–4 above. The SR original value equals 0.965.

to their share in the CC. The results of this study are found to be quite robust against small changes of the input parameters.

6 Conclusions

Cleaning action in a solar field has a significant effect on the profits of a CSP project over its lifetime. Cleaning costs (CC) correspond to 1–3% of the profits, which in turn highly depend on the efficiency of the solar field. Constant cleaning strategies (CS) can increase profits by up to 1.35% relative to a reference cleaning strategy where one cleaning unit (CU) cleans the solar field in one night and one day shift (*dn*). Nightly cleaning (*n*) achieves better results in most cases than day and night cleaning. The resulting higher investment costs for more CUs in *n* are overcompensated by the higher availability of the solar field. The CS Threshold reduces CC when solar field cleanliness (ξ_{field}) is sufficiently high. It can increase the RPI by 0.36% relative to the CS Constant, although in some cases, the benefit is negligible. The CS Assisted does not result in higher maximum RPIs compared to the CS Threshold for the soiling rates measured at PSA, but it is advantageous in cases with occasional high SRs for which not enough CUs are present. The latter can be shown in a scenario where five artificial intense soiling events are introduced to the SR dataset resulting in higher RPIs for CS Assisted compared to CS Threshold.

Power plants with storage tend to tolerate wrong cleaning decisions better than those without storage. In Morocco, where labor costs are low, a higher cleaning frequency pays off better than in Spain despite the higher Spanish feed-in tariff. Constant, daily cleaning strategies result in higher profit in Morocco as compared to Spain.

If a constant SR or constant ξ_{field} is assumed, significant errors were found by comparison to the time-resolved simulations of this work. If the constant SR is set to the mean of the reference SR-dataset, the potential increase of 0.22% on profits for the CS Threshold is not detected. If ξ_{field} is set to the mean ξ_{field} obtained with the reference CS, the profits differ by 0.58% from that with a time-resolved ξ_{field}. This represents the accuracy increase achieved with the time-resolved simulation of cleaning and soiling for the investigated case. Therefore, the here presented method increases the accuracy of yield analysis studies.

The CSs, cost parameters, and power plant layouts investigated in this study are to be understood as examples. The presented method allows for the simulation of more elaborate or custom CSs that can be investigated in future publications and that can serve as a basis for optimizing the cleaning strategies in commercial power plants.

Nomenclature

a = year
d = day
dn = cleaning action performed in one daily and one nightly shift
D_y = mean annual net dividends
$D_{y,\text{ref}}$ = mean annual net dividends for the reference cleaning strategy
D_{wocl} = dividends without considering cleaning costs
IP = power plant layout following the template "Ibersol Puertollano" plant
K_{CU} = cost for one cleaning unit
K_L = salary for one person year of solar field labor
K_L^{as} = wage for short term contract solar field labor
n = cleaning action only performed in one night shift
N_{CU} = number of cleaning units

N_{loops} = number of collector loops in a solar field
$N_{l,\text{cl}}$ = number of loops cleaned with cleaning units
$N_{l,\text{cl}}^{\text{as}}$ = number of loops cleaned by additional cleaning teams
P_F = cost of fuel for cleaning one collector loop
P_L^{as} = cost of short term contract labor for the cleaning of one loop
P_W = cost of water for cleaning one collector loop
Q_{dump} = dumped thermal energy
Q_{tot} = total thermal energy from solar field
S = availability vector for the solar field
S_i = availability of loop i
t = time
t_d = day of the year
t_n = cleaning action is performed in one night and one day shift
T_d = length of the solar day t_d
T_{lt} = total lifetime of a power plant
ξ = cleanliness
ξ_i = cleanliness of loop i
ξ_{field} = average solar field cleanliness
ξ_{lim} = threshold for ξ_{field} in CS threshold
$\xi_{\text{lim,as}}$ = threshold for ξ_{field} in CS assisted determining when external personnel is employed additional to CUs
ξ_0 = average mirror cleanliness after the passage of a CU
ρ = specular reflectance

Abbreviations

API = absolute net profit increase. Difference between the profits obtained with a candidate CS and the reference CS in EUR
AS = power plant layout similar to "Andasol I" plant
CC = cleaning costs
CS = cleaning strategy, a set of rules defining when and how cleaning is performed
CSP = concentrating solar power
CU = cleaning unit, the entity of a cleaning vehicle and operating personnel
DLR = Deutsches Zentrum für Luft- und Raumfahrt, German Aerospace Center
DNI = direct normal irradiance
ES = Spain
IP = power plant layout similar to "Ibersol Puertollano" plant
LCOE = levelized cost of electricity
MOR = Morocco
O&M = operation and maintenance
PSA = Plataforma Solar de Almería
RPI = relative profit increase of a candidate CS compared to the reference CS for same power plant layout and site
SR = soiling rate
TraCS = tracking cleanliness sensor for soiling rate measurement

References

[1] Crawford, J., Stewart, J., and Pérez-Ullivarri, J., 2012, "A Comparison of Three Portable Reflectometers for Use in Operations and Maintenance of CSP Plants," SolarPACES Conference, Marrakech, Morocco, Sept. 11–14, pp. 223–230.

[2] Deffenbaugh, D. M., Green, S. T., and Svedeman, S. J., 1986, "The Effect of Dust Accumulation on Line-Focus Parabolic Trough Solar Collector Performance," Sol. Energy, **36**(2), pp. 139–46.

[3] Biryukov, S., Faiman, D., and Goldfeld, A., 1999, "An Optical System for the Quantitative Study of Particulate Contamination on Solar Collector Surfaces," Sol. Energy, **66**(5), pp. 371–78.

[4] Pettit, R., Freese, J., E., and Roth, E., 1981, "Studies of Dust Accumulation on Solar-Mirror Materials," Sandia National Labs, Albuquerque, NM, Report Nos. SAND-81-0075C and CONF-810137-1.

[5] Fernandez-Garcia, A., 2012, *Estudio De La Reflectancia Especular En Plantas De Captadores Solares Cilindroparabolicos*, Centro De Investigaciones Energéticas, Medioambientales Y Tecnológicas (Ciemat), CIEMAT, Madrid, Spain.

[6] Griffith, D., Vhengani, L., and Maliage, M., 2014, "Measurements of Mirror Soiling at a Candidate CSP Site," Energy Procedia, **49**, pp. 1371–1378.

[7] Tahboub, Z., Dahleh, B., and Goebel, O., 2011, "Solar Mirrors Soiling Campaign Abu Dhabi," Solar Power and Chemical Energy Systems (SolarPACES), Granada, Spain, Sept. 20–23.

[8] Vivar, M., Herrero, R., Antón, I., Martínez-Moreno, F., Moretón, R., Sala, G., Blakers, A. W., and Smeltink, J., 2010, "Effect of Soiling in CPV Systems," Sol. Energy, **84**(7), pp. 1327–1335.

[9] Wolfertstetter, F., 2016, "Auswirkungen Von Verschmutzung Auf Konzentrierende Solarthermische Kraftwerke/Effects of Soiling on Concentrating Solar Power Plants," Ph.D. thesis, RWTH Aachen, Aachen, Germany.

[10] Sarver, T., Al-Qaraghuli, A., and Kazmerski, L. L., 2013, "A Comprehensive Review of the Impact of Dust on the Use of Solar Energy: History, Investigations, Results, Literature, and Mitigation Approaches," Renewable Sustainable Energy Rev., **22**, pp. 698–733.

[11] Costa, S. C., Diniz, A. S. A., and Kazmerski, L. L., 2016, "Dust and Soiling Issues and Impacts Relating to Solar Energy Systems: Literature Review Update for 2012–2015," Renewable Sustainable Energy Rev., **63**, pp. 33–61.

[12] Mani, M., and Pillai, R., 2010, "Impact of Dust on Solar Photovoltaic (PV) Performance: Research Status, Challenges and Recommendations," Renewable Sustainable Energy Rev., **14**(9), pp. 3124–3131.

[13] Kattke, K., and Vant-Hull, L., 2012, "Optimum Target Reflectivity for Heliostat Washing," SolarPACES Conference, Marrakech, Morocco, Sept. 11–14.

[14] Cohen, G. E., Kearny, D., and Gregory, J., 1999, "Final Report on the Operation and Maintenance Improvement Program for Concentrating Solar Power Plants," Sandia National Lab, Albuquerque, NM, Report No. SAND99-1290.

[15] Heimsath, A., Heck, M., Morin, G., Kiewitt, W., and Platzer, W., 2010, "Soiling of Aluminum and Glass Mirrors Under Different Climatic Conditions and Techno-Economic Optimization of Cleaning Intervals," SolarPACES, Perpignan, France, Sept. 21–24.

[16] Dersch, J., 2016, "Greenius User Manual, Version 4.1," DLR, Cologne, Germany, accessed Mar. 2017, http://freegreenius.dlr.de/images/greeniusdata/Greenius-Manual_4_1.pdf

[17] Dersch, J., and Dieckmann, S., 2015, "Techno-Economic Evaluation of Renewable Energy Projects Using the Software Greenius," Int. J. Therm. Environ. Eng., **10**(1), pp. 17–24.

[18] Quaschning, V., Ortmanns, W., Kistner, R., and Geyer, M., 2001, "Greenius: A New Simulation Environment for Technical and Economical Analysis of Renewable Independent Power Projects," Solar Forum, Washington, DC, Apr. 21–25, pp. 413–418.

[19] Blair, N., Dobos, A., Freeman, J., Neises, T., Wagner, M., Ferguson, T., Gilman, P., and Janzou, S., 2014, "System Advisor Model, Sam 2014.1. 14: General Description," National Renewable Energy Laboratory, Golden, CO, Report No. NREL/TP-6A20-61019.

[20] Wolfertstetter, F., Pottler, K., Alami, A., Mezrhab, A., and Pitz-Paal, R., 2012, "A Novel Method for Automatic Real-Time Monitoring of Mirror Soiling Rates," SolarPACES, Marrakech, Morocco, Sept. 11–14.

[21] Wolfertstetter, F., Pottler, K., Geuder, N., Affolter, R., Merrouni, A., Mezrhab, A., and Pitz-Paal, R., 2014, "Monitoring of Mirror and Sensor Soiling With Tracs for Improved Quality of Ground Based Irradiance Measurements," Energy Procedia, **49**, pp. 2422–2432.

[22] Schüler, D., Wilbert, S., Geuder, N., Affolter, R., Wolfertstetter, F., Prahl, C., Röger, M., Schroedter-Homscheidt, M., Abdellatif, G., Allah Guizani, A., Balghouthi, M., Khalil, A., Mezrhab, A., Al-Salaymeh, A., Yassaa, N., Chellali, F., Draou, D., Blanc, P., Dubranna, J., and Sabry, O. M. K., 2016, "The Ener-MENA Meteorological Network–Solar Radiation Measurements in the MENA Region," AIP Conf. Proc., **1734**(1), p. 150008.

[23] Geuder, N., Wolfertstetter, F., Wilbert, S., Schüler, D., Affolter, R., Kraas, B., Lüpfert, E., and Espinar, B., 2015, "Screening and Flagging of Solar Irradiation and Ancillary Meteorological Data," Energy Procedia, **69**, pp. 1989–1998.

[24] Sengupta, M., Habte, A., Gueymard, C., Wilbert, S., and Renne, D., 2017, "Best Practices Handbook for the Collection and Use of Solar Resource Data for Solar Energy Applications," National Renewable Energy Laboratory, Golden, CO, Report No. NREL/TP-5D00-68886

[25] CSP World, 2015, "CSP World Map," Servicios Avanzados de Comunicación y Marketing SL (SACM), Sevilla, Spain, accessed Mar. 30, 2018, http://www.cspworld.org/cspworldmap

[26] Merrouni, A. A., 2013, "Estimation on Financial Parameters Such as Land Price in Morocco," Personal Communication.

[27] Pitz-Paal, R., Dersch, J., and Milow, B., 2005, "European Concentrated Solar Thermal Road-Mapping (Ecostar)," *European Commission, Coordinated Action Sustainable Energy Systems SES6-CT-2003-502578*, Cologne, Germany.

[28] Ministerio De Agricultura, Alimentacion Y Medio Ambiente, SECRETARÍA GENERAL TÉCNICA, 2016, "Encuesta De Precios De La Tierra 2015, Principales Resultados (Julio 2016)," Ministerio De Agricultura, Alimentación Y Medio Ambiente, Madrid, Spain, Report No. 280-15-227-1.

[29] Bank al Magrhib, 2016, "Bank Al Magrhib Online Monetary and Financial Statistics Database," Bank al Magrhib, Rabat, Morocco, accessed Mar. 30, 2018, http://www.bkam.ma/en

[30] European Central Bank, 2016, "Euro Area and National MFI Interest Rates (Mir): Spain," European Central Bank, Frankfurt, Germany, accessed Mar. 30, 2018, https://www.ecb.europa.eu/press/pr/stats/mfi/html/index.en.html

[31] CSP Today, 2016, "CSP Parabolic Trough Report: Cost, Performance and Key Trends," CSP Today, London, GB.

[32] NREL, 2016, "Solar Power Projects: Noor I," National Renewable Energy Laboratory, Golden, CO, accessed Mar. 30, 2018, http://www.nrel.gov/csp/solarpaces/project_detail.cfm?projectID=270

[33] Ministerio de Industria, Turismo y Comercio, 2007, "Real Decreto 661/2007, De 25 De Mayo, Por El Que Se Regula La Actividad De Producción De Energía Eléctrica En Régimen Especial," Ministerio De Industria Turismo y comercio. Madrid, Spain.

[34] Kaiser, A., 2011, "Reflektivitätsmessungen Und Waschfahrzeugauswahl in Einem Parabolrinnen-Kraftwerk ('reflectance measurements and selection of cleaning vehicles in a parabolic trough power plant')," Bachelor thesis, Hochschule München, Germany.

[35] Grupo Albatros, 2031, "Grupo Albatros CSP Cleaning Vehicles," Grupo Albatros, Seville, Spain, accessed Mar. 30, 2018, http://helioscsp.com/albatros-the-market-leader-in-mirror-cleaning-vehicles-for-csp-plants/

[36] Freise, N. J., 2013, "A Comparative Cost Analysis of Soiling Effects on CSP Mirrors Under Variable Cleaning Scenarios: Tunisia, Morocco and Spain," Bachelors thesis, Technische Universität Dresden, Dresden, Germany.

[37] Morin, G., Dersch, J., Platzer, W., Eck, M., and Häberle, A., 2012, "Comparison of Linear Fresnel and Parabolic Trough Collector Power Plants," Sol. Energy, **86**(1), pp. 1–12.

[38] Eurostat, 2014, "Monthly Minimum Wages—Bi-Annual Data," European Commission, Brussels, Belgium, accessed Mar. 30, 2018, https://data.europa.eu/euodp/data/dataset/ueV6dmX2a5OiDORmxr3w

[39] Ministry of Employment and Social Affairs, 2016, "Salaire Minimum," Rabat, Morocco, accessed Mar. 30, 2018, http://www.emploi.gov.ma/index.php/fr/component/content/article/8-travail/15-salaire-minimum.html

[40] World Bank, 2004, "Kingdom of Morocco; Recent Economic Developments in Infrastructure Water Supply and Sanitation Sector," World Bank, Washington D.C., last accessed Jan 2017, https://openknowledge.worldbank.org/handle/10986/14390

[41] World Bank, 2016, "World Bank Open Database," World Bank, Washington DC, accessed Mar. 30, 2018, http://data.worldbank.org/

[42] Bundesarbeitsgericht, 2015, "Urteil Des Bundesarbeitsgerichts Vom 9. Dezember 2015 (10 Azr 423/14) Zu (Dauer-)Nachtarbeit. Empfehlung Eines Angemessenen Zuschlags Von 25% Zum Freizeitausgleich," Bundesarbeitsgericht, ed., Erfurt, Germany.

[43] Price, H. W., and Hassani, V., 2002, "Modular Trough Power Plant Cycle and Systems Analysis," National Renewable Energy Laboratory, Golden, CO, Report No. NREL/TP-550-31240.

[44] Zaversky, F., García-Barberena, J., Sanchez, M., and Astrain, D., 2012, "Probabilistic Modeling of a Parabolic Trough Collector Power Plant–An Uncertainty and Sensitivity Analysis," Sol. Energy, **86**(7), pp. 2128–2139.

[45] Chhatbar, K., and Meyer, R., 2011, "The Influence of Meteorological Parameters on the Energy Yield of Solar Thermal Plants," SolarPACES Conference, Granada, Spain, Sept. 20–23.

[46] Price, H., 2003, "Assessment of Parabolic Trough and Power Tower Solar Technology Cost and Performance Forecasts," National Renewable Energy Laboratory, Golden, CO, Report No. NREL/SR-550-34440.